

Influence of initial and boundary conditions for ozone modeling in very complex terrains: A case study in the northeastern Iberian Peninsula

Pedro Jiménez^{a,*}, René Parra^b, José M. Baldasano^{a,b}

^a *Barcelona Supercomputing Center-Centro Nacional de Supercomputación (BSC-CNS), Jordi Girona 29, 08034 Barcelona, Spain*

^b *Laboratory of Environmental Modeling, Universitat Politècnica de Catalunya (UPC), Avda. Diagonal 647 10.23, 08028 Barcelona, Spain*

Received 3 March 2005; received in revised form 13 January 2006; accepted 21 August 2006

Available online 27 October 2006

Abstract

Initial (IC) and boundary conditions (BC) are required in order to solve the set of stiff differential equations included in air quality models. In this work, the influences of IC–BC are analyzed in the northeastern Iberian Peninsula (NEIP) by applying MM5–EMICAT2000–CMAQ. A multiscale-nested configuration has been used to generate the IC–BC. The wider domain (D1) covers an area of $1392 \times 1104 \text{ km}^2$ centered in the Iberian Peninsula. Domain 2 (D2) covers an area of $272 \times 272 \text{ km}^2$ in the NEIP (D2) with high spatial and temporal resolution. The information related to BC has been supplied to D2 through one-way nesting. Different scenarios were considered (base case, increments of +50% in ozone (O_3) IC, +50% in O_3 BC, +50% in O_3 precursors IC, +50% in O_3 precursors BC and clean BC). The impacts of the IC on a site decrease with simulation time. Focusing on the conditions within the PBL, a 48-h spin-up time is sufficient to reduce the impact factor of IC to 10% or less for O_3 since the influence of pervasive local emissions. The influences of BC are more important for areas near domain boundaries, especially in areas where the contribution of O_3 precursors is due to a short-medium range transport.
© 2006 Elsevier Ltd. All rights reserved.

Keywords: Ozone; Air quality modeling; Initial and boundary conditions; Photochemistry; Complex terrains

1. Introduction

A three-dimensional air quality model contains a set of stiff differential equations, which describe the time evolution of chemical species in the atmosphere. Initial (IC) and boundary conditions (BC) are required in order to solve these equations. IC are specified within the simulation domain at the beginning of simulation, while BC are prescribed throughout the simulation period. Ideally, IC–BC should be determined based on observations. However, such high-resolution observations are generally not available. Model studies of photochemical pollutants pertained to a limited region and over a limited time period to some degree will be affected by the assumed IC–BC.

The extent of influence will be most profound shortly after the model simulation has been initialized and close to the model boundaries. However, the impact of these conditions could depend on several factors: quenching, depositions, chemical reactions, etc.

Since IC–BC are usually specified in some extent of presumption, it is important to minimize the influence of IC–BC in the model calculations. Three general methods are used to specify IC–BC (National Research Council, 1991): (1) use the output of a larger domain simulation; (2) use the objective or interpolated techniques when applying ambient observed data; and (3) isolate simulation domain from significant sources.

Liu et al. (2001) quantified the influences of IC–BC through theoretical analysis of the governing equation and verified the results by applying SARMAP air quality model. The influence of BC, on the other hand, decreases during the

* Corresponding author. Tel.: +34 934134050; fax: +34 93340255.

E-mail address: pedro.jimenez@bsc.es (P. Jiménez).

downwind transport, and is significant to a selected site when the arrival time of boundary condition is short and the species lifetime is long. Therefore, influences of BC are more important for area near domain boundaries.

Berge et al. (2001) have indicated that the influence of IC could be minimized through spin-up or “start-up” prior to formal simulations. Influences of IC basically depend on species lifetime. Impacts of IC on a given site decrease with simulation time and significantly affect the species concentrations before the arrival of BC, and disappear after their arrival.

The species evolution in the downwind area is continuously affected by upwind BC through this spin-up process. Thus, Seinfeld and Pandis (1998) have suggested a few rules to reduce the influences of BC. First, include all the sources that may have potential effects on the given region in the simulation domain. Second, include the sources implicitly in BC; and third, apply the simulation results of larger model domain to the BC of smaller simulation domains within. This last procedure leads to the utilization of using multiscale simulations and is called multiscale-nested modeling, and allows capturing the non-linearities of atmospheric chemistry, yet conserving computational resources. Multiscale-nested models are considered the current state-of-the-science for air quality modeling (Russell and Dennis, 2000).

A description of the process of initialization and generation of BC for MM5–EMICAT2000–CMAQ through performing simulations in the entire Iberian Peninsula, and using a multiscale approach, is shown in this work. The wider domain is coupled via one-way nesting to the domain of the northeastern Iberian Peninsula (NEIP), in order to provide the BC. Furthermore, an analysis of the influences of IC–BC and their sensitivity is presented, indicating the necessity of a correct initialization of the model by means of spin-up procedures; and also the availability of good-quality boundary information when performing simulations in very complex terrains.

2. Multiscale-nested simulation approach

Indications of the National Research Council (1991), Seinfeld and Pandis (1998) and Liu et al. (2001) were followed for the NEIP, in order to minimize the impacts of IC–BC in the simulations and to maximize local characteristics. In this section, a short description of the methods used for the nested simulation is indicated.

The simulations were started at 00.00 UTC of 13 August 2000, and extend for a period of 72 h. This episode corresponds to a typical summertime low pressure gradient with high levels of photochemical pollutants over the Iberian Peninsula. The day was characterized by a weak synoptic forcing, so that mesoscale phenomena, induced by the particular geography of the region would be dominant. This situation is associated with weak winds in the lower troposphere, cloudless skies and high maximum temperatures. A high sea level pressure and almost non-existent surface pressure gradients over the domain characterize this day, with slow northwesterlies

aloft. This situation is representative of an episode of photochemical pollution in the Western Mediterranean Basin, since the occurrence of regional re-circulations at low levels represents 45% of the yearly (and 78% of summertime days) transport patterns over the area of study (Jorba et al., 2004). These situations are associated with local-regional episodes of air pollution in the NEIP that result in high levels of ozone (O_3) (Pérez et al., 2006) and an increase of particulate matter within the boundary layer during summer.

The domains selected are shown in Fig. 1. The wider domain (D1) represents an area of $1392 \times 1104 \text{ km}^2$ centered in the Iberian Peninsula, with a horizontal resolution of 24-km and 16 vertical layers to cover the troposphere. The information related to the BC has been supplied from D1 into an inner domain through a one-way nesting approach. The simulation of Domain 2 (D2) covers an inner area of $272 \times 272 \text{ km}^2$ in the NEIP. Model resolution for this second domain is 2-km horizontally, and 16 layers of variable thickness in altitude. The need for this high resolution has been highlighted by some recent works (e.g. Jiménez et al., 2005, 2006; Sokhi et al., 2006; Zhang et al., 2006), which find a tendency to underproduction of photochemical pollutants when a coarse grid is used for numerical experiments. For Catalonia, ozone concentrations over $189 \mu\text{g m}^{-3}$ are simulated for Domain 2 with MM5–EMICAT2000–CMAQ when performed nested simulations for 14 August 2000, at 12.00 UTC (Fig. 1).

2.1. MM5–CMAQ air quality model

Nowadays, the state-of-the-art air quality modeling systems (such as MM5–CMAQ used in this work) can handle the evaluation of air pollution concentrations in a very high detail in time and space (San José et al., 2007). The MM5 numerical weather prediction model (Dudhia, 1993) provided the meteorology dynamical parameters as inputs to CMAQ. MM5 physical options used for the simulations were Mellor–Yamada scheme as used in the Eta model for the PBL parameterization; Anthes–Kuo and Kain–Fritsch cumulus scheme; Dudhia simple ice moisture scheme; the cloud-radiation scheme; and the five-layer soil model. Initialization and BC for the mesoscale model were introduced with analysis data of the European Center of Medium-range Weather Forecasts global model (ECMWF). Data were available at a 1-degree resolution (100-km approx. at the working latitude) at the standard pressure levels every 6 h.

The chemical transport model used to compute the concentrations of photochemical pollutants was CMAQ (Byun and Ching, 1999). IC–BC were derived from a one-way nested simulation covering D1, which used EMEP emissions corresponding to year 2000 (www.emep.int). For the domain of the Iberian Peninsula, static IC–BC are considered. The limitation in air mass inflows in the domain due to the meteorological conditions of the episode (Jorba et al., 2004) minimizes the influence of BC in D1. The chemical mechanism selected for simulations was CBM-IV (Gery et al., 1989), including aerosols and heterogeneous chemistry. Nitrogen oxides (NO_x) and volatile organic

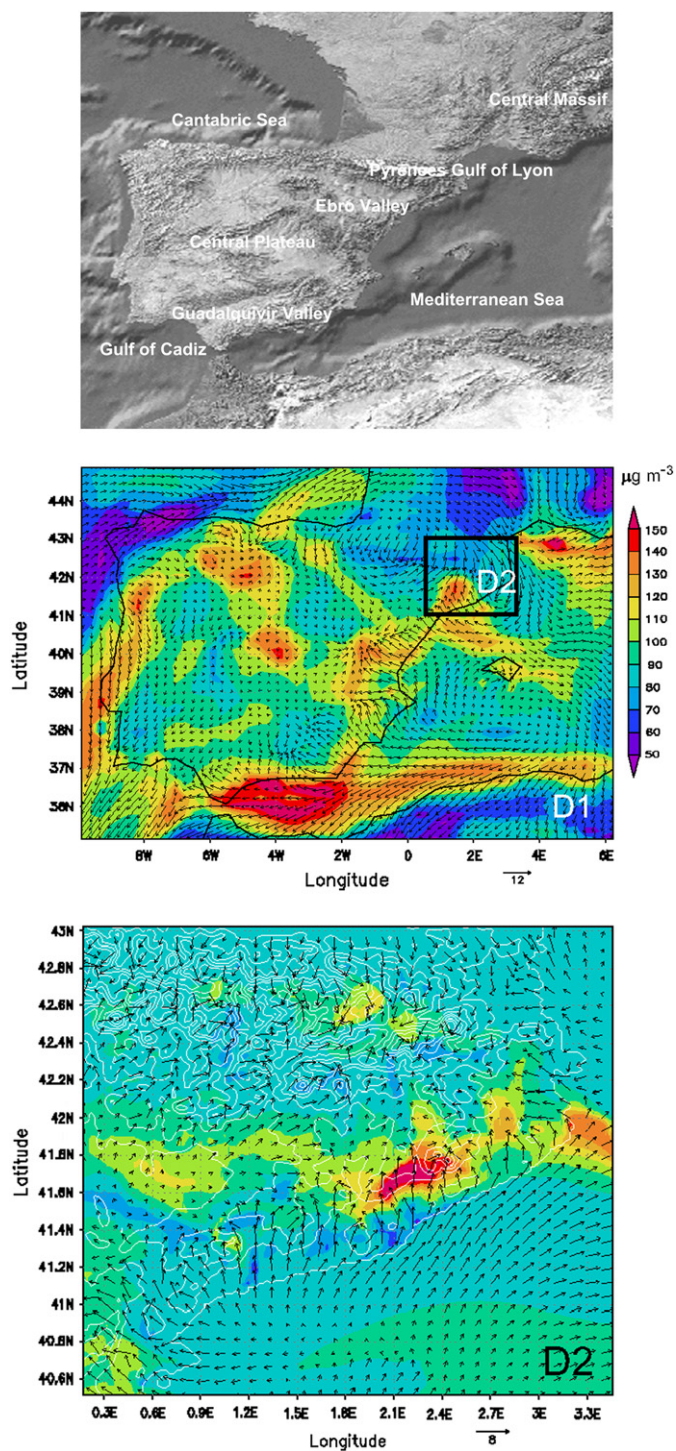


Fig. 1. (Up) Geographic features of the domain of study; (center) Ozone concentrations ($\mu\text{g m}^{-3}$) and wind field vectors (m s^{-1}) for D1 (Iberian Peninsula, northern Africa and southern France) and (bottom) D2 (northeastern Iberian Peninsula) at 12.00 UTC on 14 August 2000.

2.2. Emissions within MM5–EMICAT2000–CMAQ

Emissions used for the external domain of the Iberian Peninsula (D1) were derived from EMEP (www.emep.int) emissions database of year 2000, on an hourly basis and lumped according to Carbon Bond IV chemical mechanism (Gery et al., 1989). Chemical species considered were NO_x , non-methane volatile organic compounds (NMVOCs), sulfur dioxide (SO_2), sulfates, carbon monoxide (CO) and ammonia. The vertical distribution of emissions was implemented following EMEP national profiles. Cells from the European EMEP mesh have a resolution of 50-km in polar coordinates; but these emissions were interpolated into a grid of 24-km resolution in Lambert coordinates, as needed by the defined D1 in MM5–EMICAT2000–CMAQ. The biogenic emissions (included in EMEP sector 11) were not derived from EMEP, but estimated following the methods implemented in EMICAT2000 (Parra et al., 2004, 2006), using the land-use map derived from NATLAN2000 and the United States Geological Survey according to the methodology by Pineda et al. (2004), and adapting the resulting land-uses to the 22 categories of EMICAT2000. Meteorological data (solar radiation and temperature) were derived from the simulations for Domain 1 performed with MM5 meteorological model. The emission factors and the density of foliar biomass correspond to the results by Parra et al. (2004) for the Iberian Peninsula environment. Fig. 2 indicates the distribution of biogenic emissions of non-methane volatile organic compounds during 15 August 2000, in D1, in order to perform simulations for obtaining the IC–BC for the inner D2. Fig. 2 also depicts the distribution of the emissions at 12.00 UTC of 13 August 2000, for the species nitrogen monoxide and toluene, at surface and 150 m in altitude.

The high resolution (1 h and 1 km^2) EMICAT2000 emission model (Parra et al., 2006) has been applied in the NEIP (D2). This emission model includes the emissions from vegetation, on-road traffic, industries and emissions by fossil fuel consumption and domestic–commercial solvent use. The biogenic emissions may exert a considerable influence in ozone formation, being as important as the anthropogenic contribution in vegetation and localized crop areas (Zunckel et al., 2006). Therefore biogenic emissions were estimated using a method that takes into account local vegetation data (land-use distribution and biomass factors) and meteorological conditions (surface air temperature and solar radiation) together with emission factors for native Mediterranean species and cultures (Parra et al., 2004). On-road traffic emission includes the hot exhaust, cold exhaust and evaporative emissions using the methodology and emission factors of the European model EMEP/CORINAIR–COPERTIII (Ntziachristos and Samaras, 2000) as basis, and differencing the vehicle park composition between weekdays and weekends (Jiménez et al., 2005). Industrial emissions include real records of some chimneys connected to the emission control net of the Environmental Department of the Catalonia Government (Spain), and the estimated emissions from power stations (conventional and cogeneration units), cement factories, refineries, olefins plants, chemical industries and incinerators.

compounds (VOCs) specification of EMICAT2000 emissions, as required by CBM-IV, could be found in Parra et al. (2006). The algorithm chosen for the resolution of tropospheric chemistry was the Modified Euler Backward Iterative (MEBI) method (Huang and Chang, 2001).

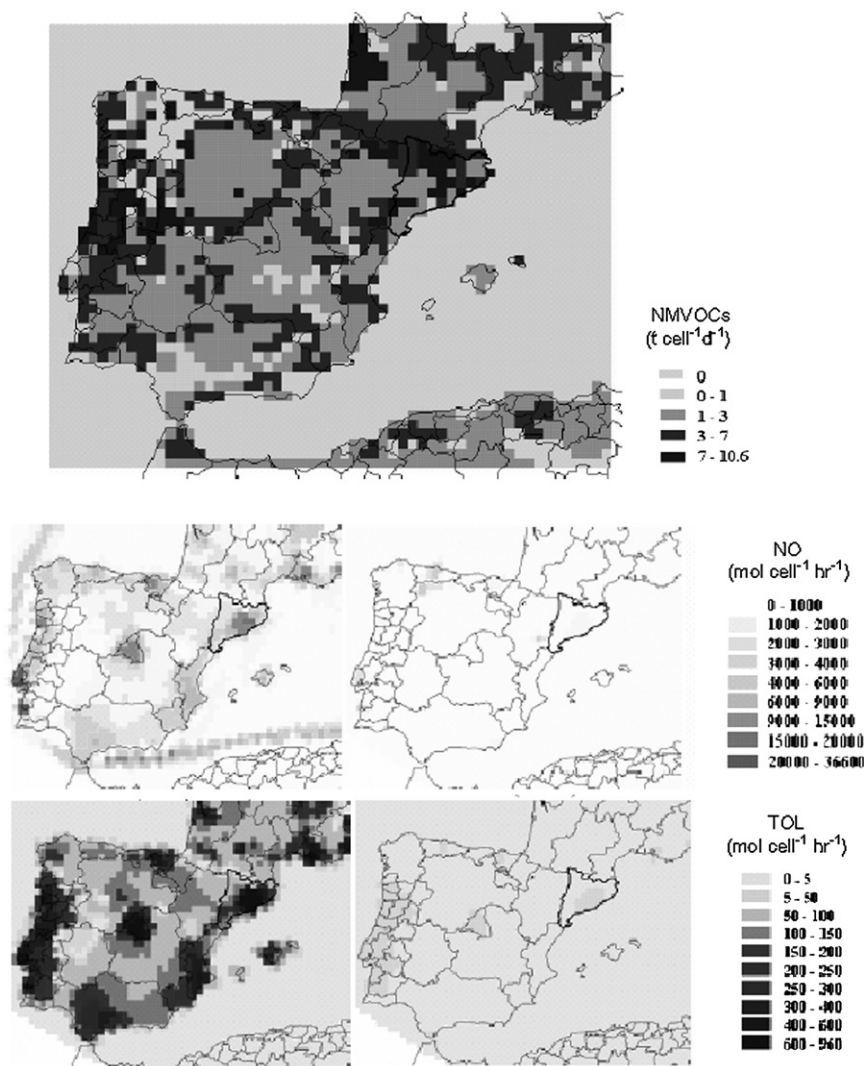


Fig. 2. Emissions for D1: map of biogenic emissions on 15 August 2000, for D1 (top); and categories NO and TOL of CBM-IV mechanism: (left) surface; and (right) 150 m height.

3. Results and discussions

Multiscale-nesting technique grids are needed to provide the required high resolution simulations. Nesting techniques allow one-way or two-way exchange of information among finer and coarser grids. The only difference between the one-way and two-way nesting is whether concentrations in coarser grid simulations are updated with the finer grid simulations through the feedback processors or not. Soriano et al. (2002) studied the influence of one-way and two-way nesting techniques over the very complex terrain of the NEIP under a situation of low synoptic forcing. The differences in the simulated fields are significant when choosing one or another nesting technique, yielding the two-way simulation worst results when evaluating the model against ambient data. Therefore, the decision of considering one-way approaches was taken for the simulations performed in this work both for MMS and CMAQ.

The evolution of the flows and the concentrations of photochemical pollutants for a daily cycle over the Iberian

Peninsula are shown in Fig. 3 for O₃ and Fig. 4 in the cases of CO and NO_x. The simulations depict the results for 14 August 2000 in the D1 (covering the Iberian Peninsula, northern Africa and southern France) since this day is representative of the episode of pollution covering from 10 to 19 August 2000, characterized by thermal circulations that dominate most of the Peninsula for these days.

The nocturnal regime is characterized by the development of mountain and katabatic winds in main orographic systems and the formation of land breezes in coastal areas. In the west littoral, flows are influenced by the anticyclonic dorsal. At night, there are three important drainages of pollutants in D1. First, the drainage through the Ebro Valley in the north-eastern part of the Peninsula is hampered by the penetration of hot air masses from the Mediterranean induced by the anticyclonic circulation over the sea. Second, flows are canalized between the Pyrenees and the Central Massif, introducing northwestern flows into the Mediterranean through the Gulf of Lyon. This canalization plays an important role, because it is the only pass bringing fresh air into the Western

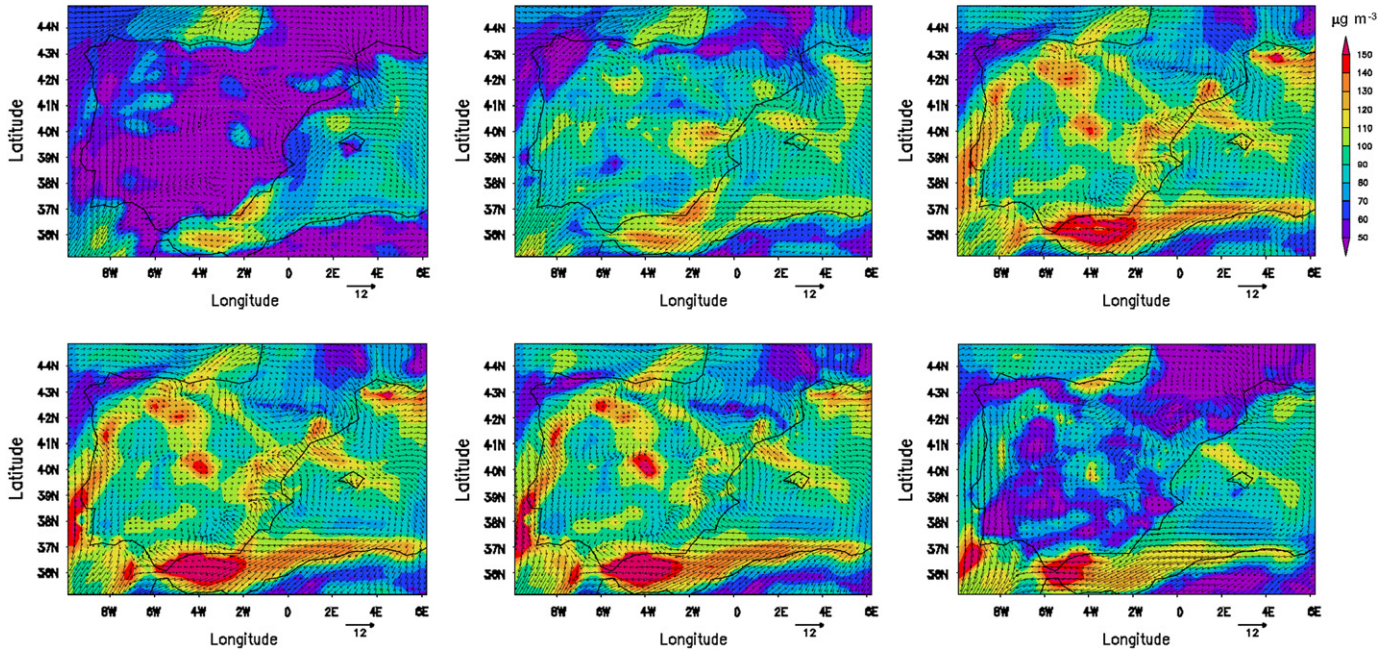


Fig. 3. Ozone concentrations ($\mu\text{g m}^{-3}$) and wind field vectors (m s^{-1}) at ground-level over D1 with MM5-EMICAT2000-CMAQ on 14 August 2000, at (from top-left to bottom-right) 06.00 UTC, 10.00 UTC, 12.00 UTC, 14.00 UTC, 16.00 UTC and 20.00 UTC.

Mediterranean Basin (Gangoiti et al., 2001). Last, polluted air masses are drained in the Guadalquivir Valley, in southwestern Iberian Peninsula, towards the Gulf of Cádiz.

The diurnal regime is observable from 08.00 UTC, with the establishment of sea breezes on the coast; and valley and anabatic winds in orographic systems. At 10.00 UTC, the breeze has a component S-SE in the northeastern littoral of the Iberian Peninsula, E in the southern littoral and NW-N

in the northern coast. The sea flows penetrate through orographic canalizations, reinforced with thermal diurnal circulations and the anabatic winds in the coastal mountain ranges.

Millán et al. (1992) define the behavior of breezes in the Western Mediterranean Coast as a coalescence of the breeze circulation with other thermal circulations, originating a “macro-breeze” when the breeze cell joins the convective cell developed in the central plateaus. Pérez et al. (2004)

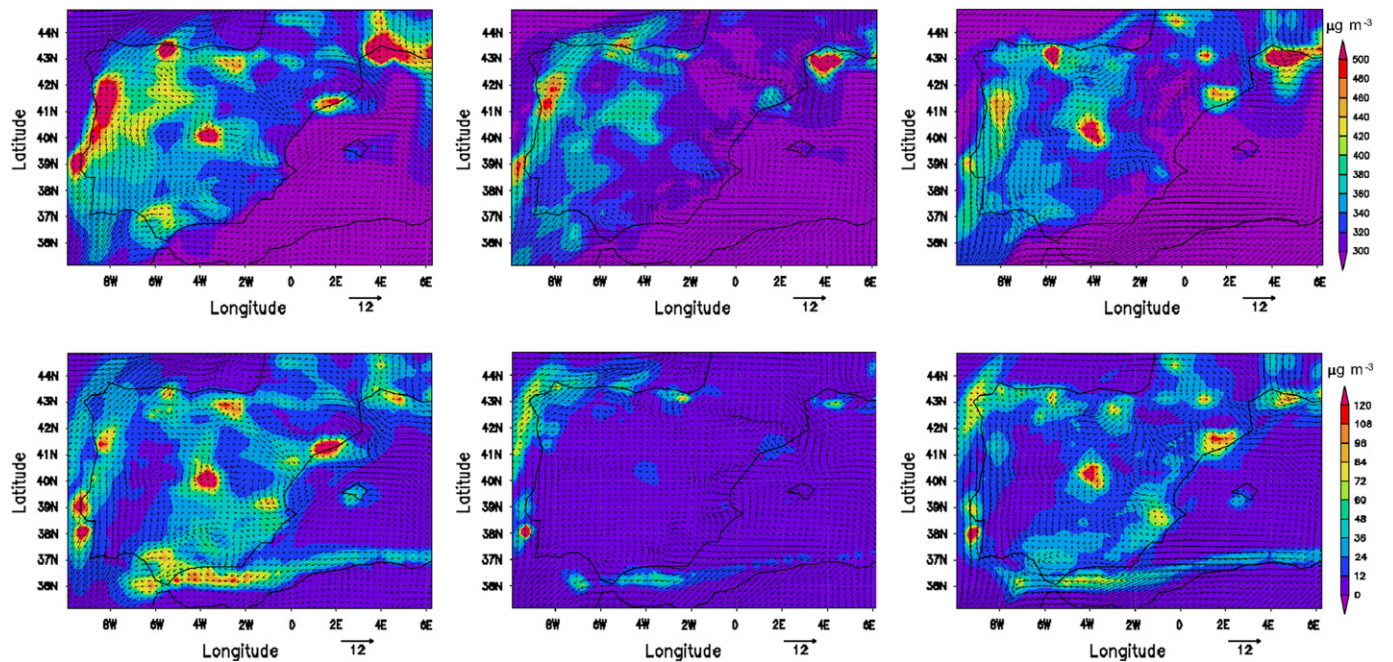


Fig. 4. Carbon monoxide (top) and nitrogen oxides concentrations (bottom) both in $\mu\text{g m}^{-3}$; and wind field vectors (m s^{-1}) at ground-level over D1 with MM5-EMICAT2000-CMAQ on 14 August 2000, at (from left to right) 06.00 UTC, 12.00 UTC and 20.00 UTC.

have corroborated these processes in the eastern coast of the Iberian Peninsula by using numerical weather prediction models.

The surface heating during daytime hours and the convergence of flows inland the Iberian Peninsula produces the development of the Iberian Thermal Low (Millán et al., 1992, 1996, 1997), which leads to very weak circulations in the central Plateau. The maximum development of the Iberian Thermal Low is observed around 18.00 UTC. The pressure gradient in the central Plateau of the Iberian Peninsula is negligible. From 20.00 UTC, flows weaken and the nocturnal regime dominates the dynamics of air pollutants. Drainages are developed in main valleys and peninsular orographic systems.

In order to assess the influence of IC–BC in tropospheric O₃ levels, different simulations were performed in D2 by modifying the IC–BC generated from the nested simulation of D1. Apart from the base case, five different scenarios were defined: (1) Scenario 1: increase of +50% in O₃ IC; (2) Scenario 2: +50% in O₃ precursors' IC; (3) Scenario 3: increase of +50% in O₃ BC; (4) Scenario 4: +50% in O₃ precursors' BC; and (5) Scenario 5: clean BC.

3.1. Influence of initial and boundary conditions

Four representative sites are selected to highlight the sensitivities to IC–BC (Fig. 5), attending to their proximity to the different boundaries, their different sensitivity to NO_x and VOCs emissions (Jiménez and Baldasano, 2004) and their characteristics. Therefore, Sites 1 (Sort) and 4 (la Sénia) are background scenarios where the influence of IC–BC is higher than in urban locations (Site 2, Vic, and Site 3, Barcelona), where the local emissions-photochemistry cycle may play a more important role. For these scenarios and sites, the basic features of the evolution of O₃ and the affected response by

modifying the IC–BC in MM5–EMICAT2000–CMAQ is represented.

In Fig. 6, the arrival time of BC varied with the selected sites depending on their distance to the upwind boundary condition. The arrival times of BC were 22, 36, 24 and 1 h for Sites 1–4, respectively. For a same species, longer arrival time of BC allows more time for simulated tracers to decay further during the transport processes and results in a weaker influence of BC (Liu et al., 2001).

The impacts of both IC–BC may fluctuate with time during the simulation period (Fig. 6). The fluctuations are caused by the different behavior of emissions and wind fields during the episode selected. The percentual difference between Scenario 1 (+50% O₃ in IC) and the base case shows a secondary maximum in urban sites (Site 2: Vic and Site 3: Barcelona) after 29–30 h of the beginning of the simulation, with deviations exceeding the 50%. After this maximum, a sudden decrease is produced, being the impact factor under 10% after approximately 40 h. A possible explanation of these variations is found in Liu et al. (2001), where it is indicated that different heights of mixing layer between day and night also lead to fluctuated differences between diverse scenarios.

The impact factor for increasing the initial or boundary concentrations of precursors (Scenarios 2 and 4, respectively) remains under 15% for all the period of simulation, and is negligible after 36 h of spin-up time. It should be highlighted that, for Site 4 (la Sénia), Scenario 4 leads to slightly higher decreases of O₃ concentrations at night respect to the base case, because of a higher O₃ depletion throughout the reaction with NO introduced by BC. On the other side, this increase in precursors makes O₃ concentrations exceed the levels of the base case on a 15–20% during the hours of daylight. However, this pattern is not observed in other sites further from boundaries. Ozone in Scenario 4 increases rapidly after 36 h of simulation to a 10% difference respect to the base case and progressively reaches a 20% difference 72 h after the start of the study for Site 3 (Barcelona). Because of the lack of anthropogenic emissions in background areas, the proximity of la Sénia to the south and western boundary makes the difference between the Scenario 3 (+50% O₃ in boundaries) and the base case reach 50% after just 4 h of the start. This impact factor remains practically constant during the simulation period; therefore, the transport of external pollutants through the boundaries dominates the levels of O₃ in this location, as discussed later for simulations with clean BC.

In comparison with the influence of BC, the impact of IC decays approximately in an exponential way and presents an anti-correlated behavior respect to the BC. Focusing on processes within the boundary layer, a 48-h spin-up time is sufficient to reduce the impact factor of IC to 10% or less for O₃ in all sites, both when incrementing O₃ or precursors in the boundary concentrations. On the other side, the impact factor is controlled by the BC after a certain time of simulation, related to the arrival of upwind air masses. This impact factor for BC stabilizes around 50% after 48 h for Sites 1, 3 and 4, and fluctuates in the simulations for Site 2, achieving a factor of 70% 72 h after the start of simulations.

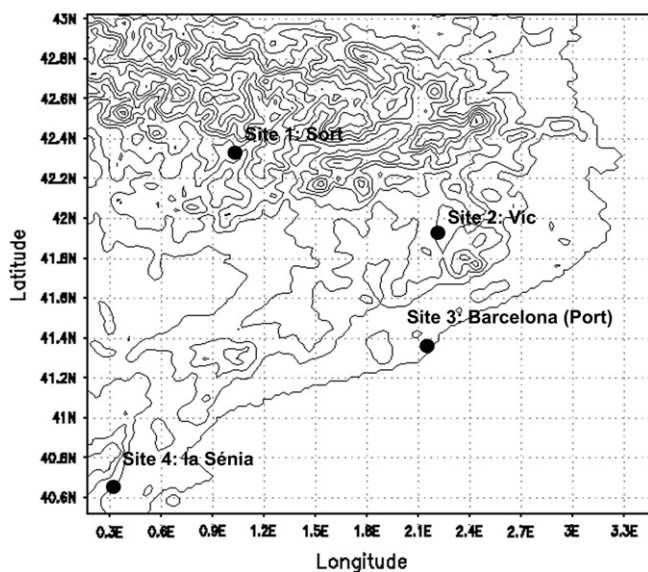


Fig. 5. Location of sites within D2 included in the analysis of the influence of IC–BC.

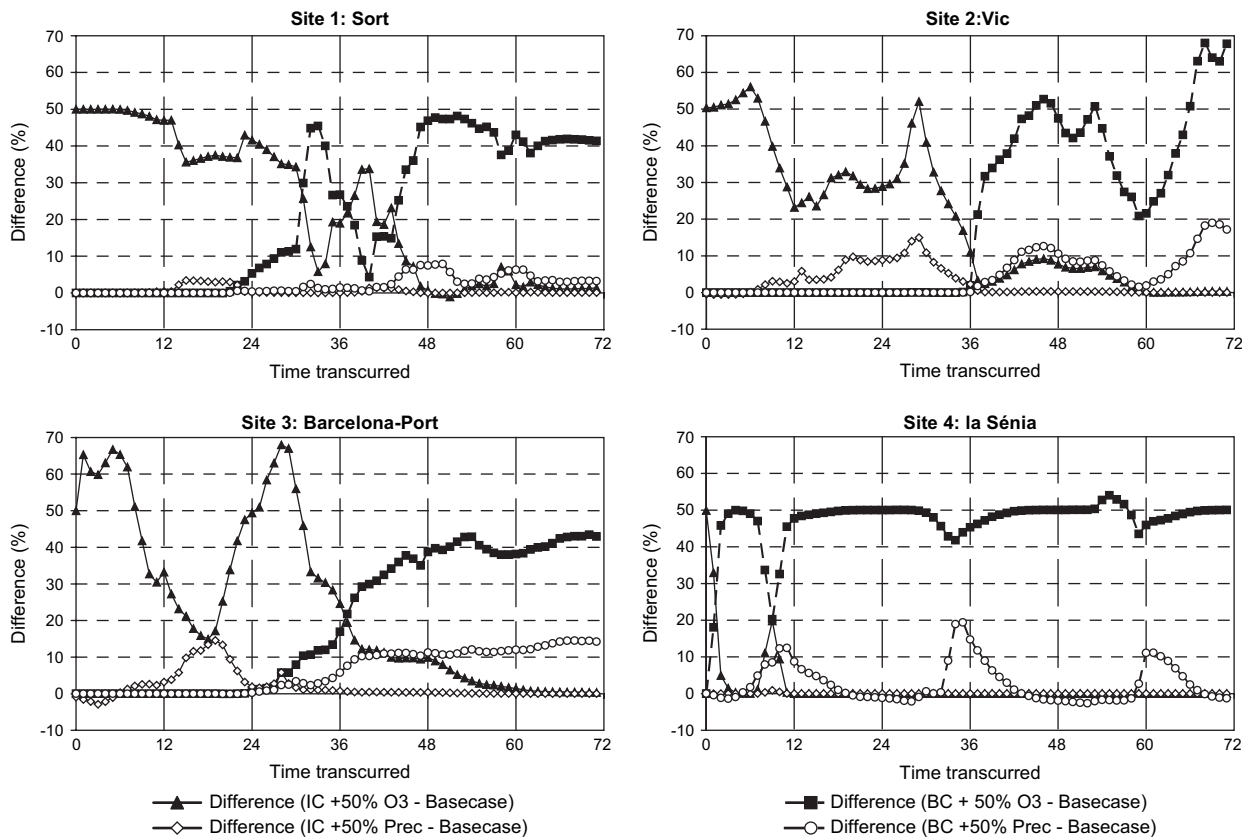


Fig. 6. Evolution of the differences in ground-level ozone concentrations (%) for the sites defined in Fig. 5.

It is also noteworthy that the influence of IC can still remain significant when the air parcel from the boundary arrives. Therefore, the start-up helps reducing the influence of IC, but it also introduces the influence of boundary condition in the case of O_3 . For other species with longer lifetime, Berge et al. (2001) report that this fact is especially true for the upper troposphere, since lifetimes of chemical species there are usually longer.

The impacts of IC on the estimated results by MM5–EMICAT2000–CMAQ for the entire domain of the NEIP are illustrated in Fig. 7 for Scenario 1 (+50% O_3 in IC) and Fig. 8 for Scenario 2 (+50% precursors in IC). In the case of Scenario 1, differences in O_3 concentrations at the beginning of the simulation are specially important over the areas with higher O_3 levels at night that are mainly rural areas (e.g. the Pyrenees, etc.) and the Mediterranean Sea. After 24 h of simulations, differences are minimized over the northern, western and southern parts of D2, where O_3 concentrations are conditioned by the transport through the boundaries, which remain equal for Scenario 1 and base case.

At this time, the impact of IC is important over the Pyrenees and the tongue-shaped area covering coastal sites, where the emissions-photochemistry cycle plays an important role and gets more affected because of IC. The influence in O_3 levels may achieve $30 \mu\text{g m}^{-3}$ in the littoral of the NEIP (Fig. 7). Inland, these variations are in the order of $20\text{--}25 \mu\text{g m}^{-3}$. However, after 48 h of the beginning, the differences between Scenario 1 and the base case have reduced to

approximately $15 \mu\text{g m}^{-3}$ in the sub-Pyrenees and $5 \mu\text{g m}^{-3}$ in coastal sites. The rest of the domain presents no important variances with respect to the base case, which are negligible when a spin-up time of 72 h is considered.

The differences between the base case and the Scenario 2 (Fig. 8) are negligible for O_3 concentrations at the beginning of the simulation. Afterwards, main differences are observed in the photochemically aged masses departing from the city of Barcelona, where an increase in the concentrations of precursors at the start of simulations leads to a higher formation of O_3 during the hours of photochemical activity. However, these air masses with a higher concentration of O_3 and precursors with respect to the base case are transported by mesoscale flows during the development of the sea–land breezes cycles, extracting them from the area of study (as observed in the northeastern limit of the domain after 24 h of simulation).

Once this O_3 -rich air mass, as a consequence of +50% of precursors in IC, has been extracted from D2, the local emissions (which remain the same for Scenario 2 and base case) dominate the photochemical cycle and the impact is negligible after 48–72 h of the beginning of the simulation.

Fig. 9 for Scenario 3 (+50% O_3 in BC) and Fig. 10 in the case of Scenario 4 (+50% precursors in BC) demonstrate that if the arrival time of the BC is small, then the O_3 concentrations are significantly affected by the value of BC; when the arrival time of BC is large, influences of IC–BC are greatly reduced due to the decaying effects, and the estimated O_3 concentrations are mainly contributed by the local and upwind

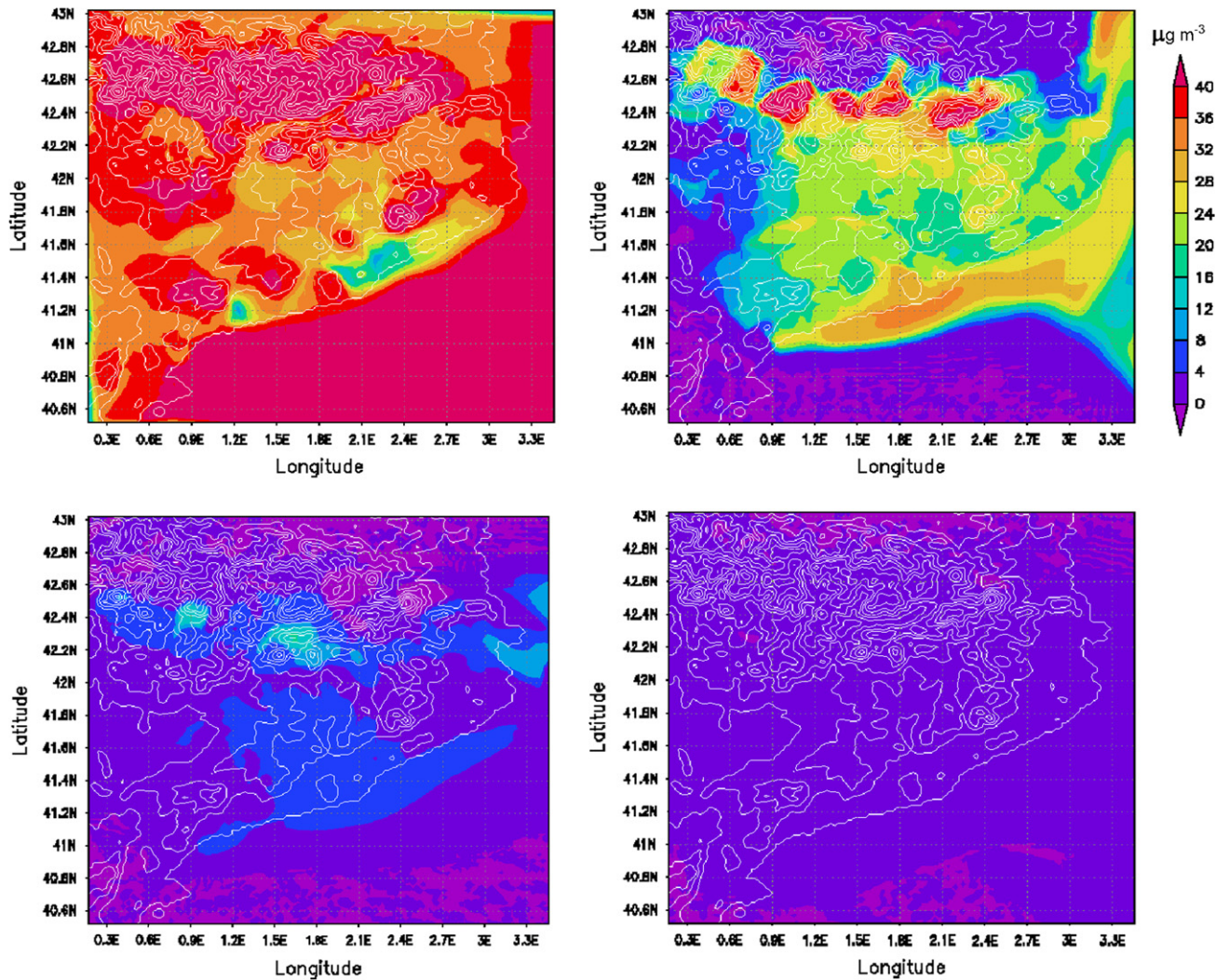


Fig. 7. Difference in ground-level ozone ($\mu\text{g m}^{-3}$), Scenario 1 (+50% in ozone IC) – base case after 0, 24, 48 and 72 h of the beginning of simulation.

characteristics. The difference of O_3 concentration progressively increases during the simulation. In Scenario 3 (Fig. 9), after 24 h, minimal differences are observed between Scenario 3 and the base case.

The concentrations of O_3 that are $40 \mu\text{g m}^{-3}$ higher than those of the base case are found over the Mediterranean Sea in the southern part of the domain and in the Pyrenees in Scenario 3 that remain practically constant during the 72 h of simulation. Pollutants (mainly, photochemically aged air masses with high concentrations of O_3 and poor in photochemical precursors) are transported towards the Mediterranean area, where they sink within the anticyclone located over the Western Mediterranean Sea (Gangoiti et al., 2001). A fraction of these pollutants are advected out from the domain of the NEIP, and the other fraction is incorporated on the following morning to the sea breeze cycle. This transport through the southern boundary indicates a reservoir layer of O_3 that remains over the Mediterranean Sea during the episode considered (which can be observed in Fig. 3). The development of sea breezes' cycles re-circulates these air masses again into the domain of the NEIP. Furthermore, the transport of

pollutants with a peninsular origin through the western boundary may have a certain importance in sites near this boundary ($25 \mu\text{g m}^{-3}$ after 48 h and around $35 \mu\text{g m}^{-3}$ in the western boundary). Last, in the middle of the domain, boundaries arrive after approximately 20–30 h after the beginning of the simulation, depending on the site, and differences of Scenario 3 with respect to the base case reach $30 \mu\text{g m}^{-3}$ inland the NEIP after 72 h.

For Scenario 4 (Fig. 10), the main transport of precursors appears to be produced through the western boundary (Peninsular origin) that produces increments in O_3 concentrations around $20 \mu\text{g m}^{-3}$ in Plana de Lleida and $15 \mu\text{g m}^{-3}$ in the Mediterranean Sea after 24 h of simulation. The reservoir layer over the Mediterranean is poor in precursors (as observed in Figs. 4 and 5 for the simulation of precursors of the D1), and therefore southern boundary does not seem to present a relevant influence on O_3 concentrations on the following days. After 48 h, the westerly winds have transported precursors over the littoral mountains, and they influence all the coastal line and the Mediterranean Sea with differences with respect to the base case over $15\text{--}20 \mu\text{g m}^{-3}$. Finally, after

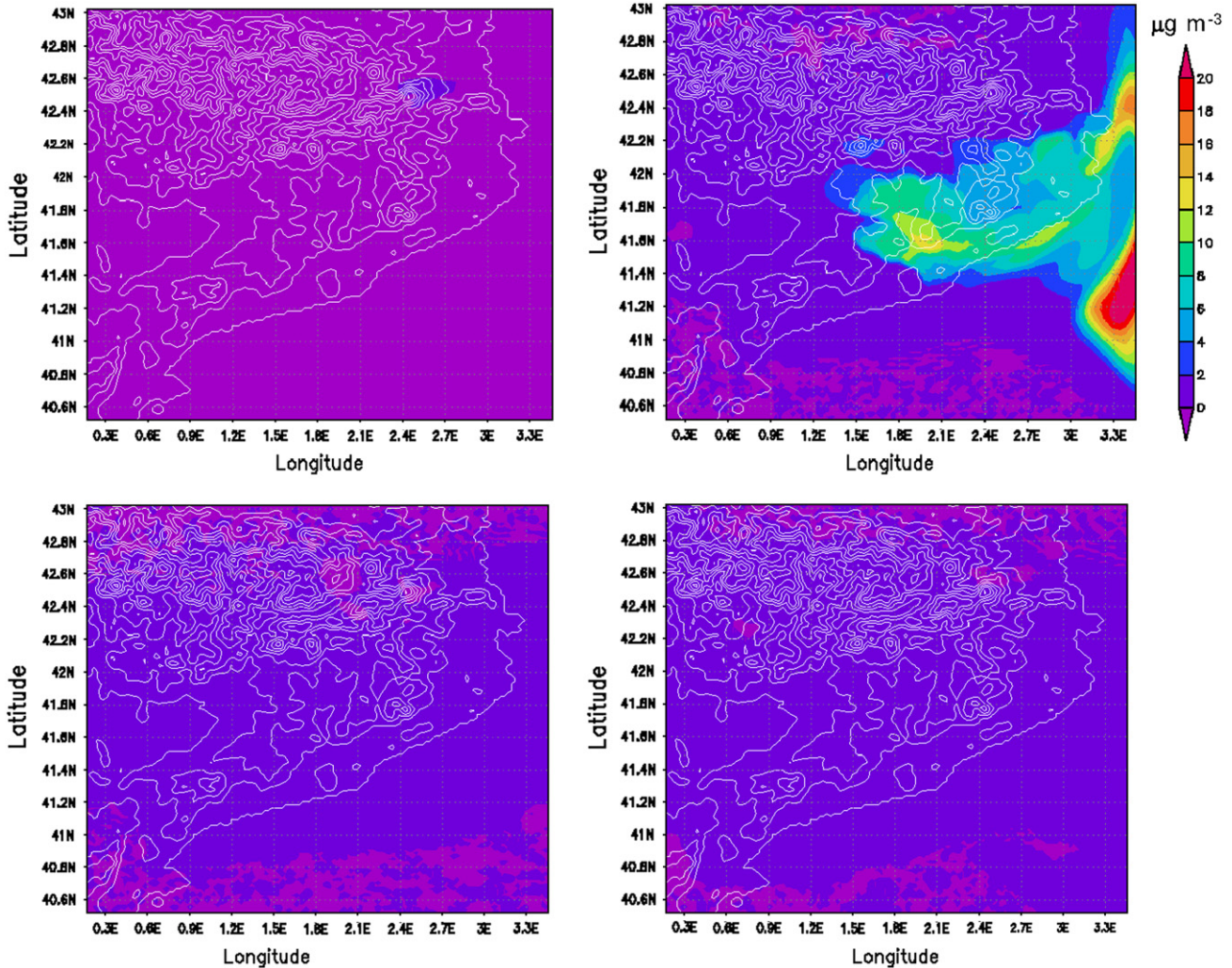


Fig. 8. Difference in ground-level ozone ($\mu\text{g m}^{-3}$), Scenario 2 (+50% in IC of precursors) – base case after 0, 24, 48 and 72 h of the beginning of simulation.

72 h concentrations in the central plateaus and the southeastern part of domain are controlled by the participation of precursors introduced through the boundaries into the domain.

3.2. Analysis of advective transport by using clean BC

In order to account for the contribution of advective transport through the BC to O_3 levels, simulations with MM5–EMICAT2000–CMAQ for D2 were conducted with clean BC with respect to the base case simulations (Scenario 5). These results within the boundary layer are shown in Fig. 11 for 1 h-maximum and daily average O_3 levels.

The modeled O_3 with MM5–EMICAT2000–CMAQ indicates that the most important influence of advective transport on O_3 (both for 1 h-maximum concentration and average levels) is produced over the Mediterranean Sea. Maximum simulated 1 h O_3 is achieved downwind the city of Barcelona, in latitude 41.842 N and longitude 2.305 E ($189.1 \mu\text{g m}^{-3}$ in the base case, and $184.4 \mu\text{g m}^{-3}$ in Scenario 5). Therefore, the contribution of advective transport to maximum O_3 levels is $4.7 \mu\text{g m}^{-3}$, which involves a 2.5% of the final maximum

concentrations. As shown in Fig. 3, there is an important reservoir of O_3 over the Western Mediterranean coast and the Balearic Islands, which is transported to D2 through the southern boundary with the development of the sea breeze. This O_3 accounts for $90 \mu\text{g m}^{-3}$; however, the dominant chemistry in the Levantine coast of the NEIP is dominated by local photochemistry. In coastal areas, the strong forcing of emissions is the most relevant process, having the advective transport an importance of 5–10% (around $10 \mu\text{g m}^{-3}$) with respect to maximum O_3 levels in these areas. The contribution to daily average levels is more important, around 30% in these areas ($20 \mu\text{g m}^{-3}$) since of the vertical descend of O_3 reservoir layers during the night as a consequence of the compensatory subsidence (Pérez et al., 2004), which introduces O_3 in the lower troposphere and the PBL.

In addition, the transport through the western boundary (air with an origin set in the Iberian Peninsula) may contribute to the 1 h peak levels achieved in the plain of Lleida with $50 \mu\text{g m}^{-3}$. In this area, due to the lack of anthropogenic emissions, the advective transport represents over 70% of the O_3 within the PBL, importantly contributing to background levels.

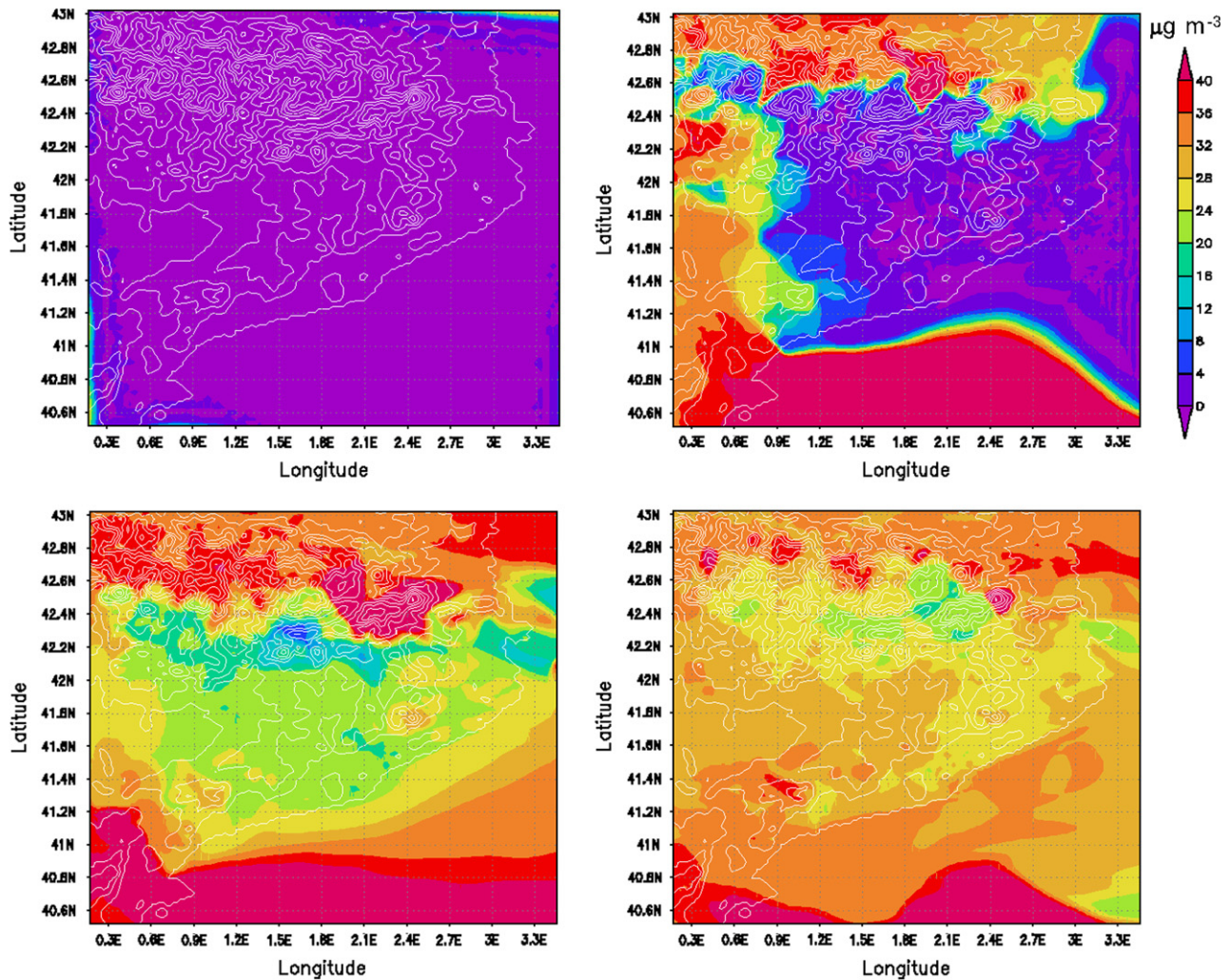


Fig. 9. Difference in ground-level ozone ($\mu\text{g m}^{-3}$), Scenario 3 (+50% in ozone BC) – base case after 0, 24, 48 and 72 h of the beginning of simulation.

With respect to average daily levels, the advective transport of air masses through the western boundary is responsible for nearly the 90% of the O_3 in the western domain of study, contributing with $60\text{--}70 \mu\text{g m}^{-3}$ to the O_3 photochemically produced in the area. The origin of these air masses may be explained by the peninsular transport of polluted air masses and the polluted air masses from the industrial area of Castellón that, due to the anticyclonic circulations, enter in D2 throughout the south and western boundaries. The influence of northern boundary condition on O_3 concentrations in the northern slope of the Pyrenees (air masses with a background origin from Atlantic Ocean and southern France) is also important; here, the transport of ozone from outside D2 could account for over 90% of both average and 1-h peak concentrations.

3.3. Model evaluation

Despite a surface measurement represents a value only at a given horizontal location and height, while the concentration predicted by the model represents a volume-averaged value, performance of the model was statistically evaluated by comparing the first-layer simulations results and the values measured in the

meteorological and air quality stations of the domain under study. Air quality stations hourly data averaged over the study domain were used in order to report evaluation parameters for CMAQ. Hourly measures of ground-level O_3 were provided by 48 air quality surface stations which belong to the Environmental Department of the Catalonia Government (Spain).

The US Environmental Protection Agency has developed guidelines for models performance (USEPA, 1991, 2005). Those statistics are: mean normalized bias error (MNBE), mean normalized gross error for concentrations above a prescribed threshold (MNGE), and unpaired peak prediction accuracy (UPA). Observation/prediction pairs were excluded from the analysis when the observed concentration was below a cut-off level of $120 \mu\text{g m}^{-3}$ (Hogrefe et al., 2001). These discrete statistics measure the skill of the model when performing diagnostic analyses of pollutant concentrations at specific points (where air quality stations are located). Categorical statistics as derived from Kang et al. (2003, 2004) have also been used to evaluate the different vertical and horizontal grid spacing, including parameters such as the model accuracy (A), bias (B), probability of detection (POD), false alarm rates (FAR) and critical success index (CSI).

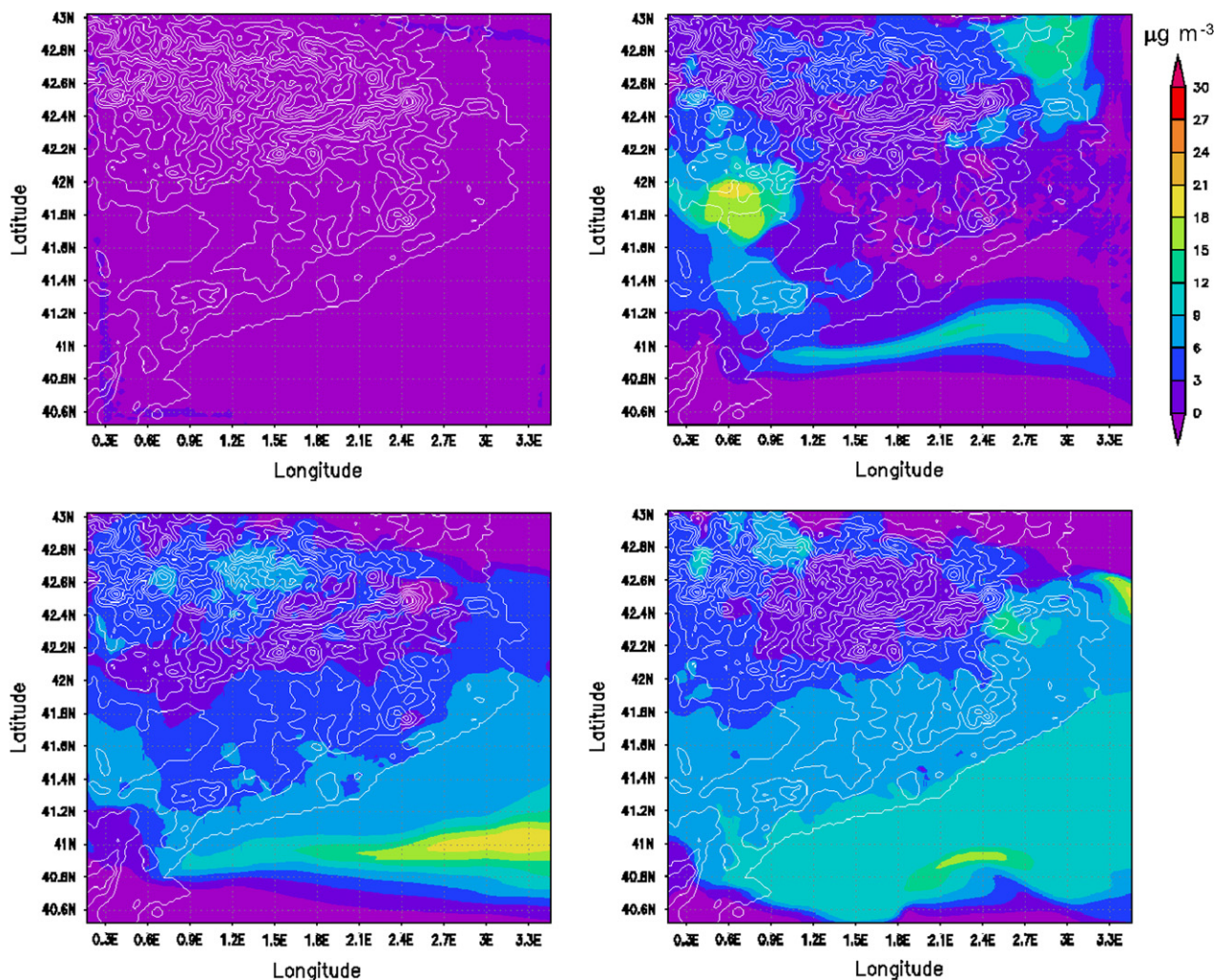


Fig. 10. Difference in ground-level ozone ($\mu\text{g m}^{-3}$), Scenario 4 (+50% in BC of precursors) – base case after 0, 24, 48 and 72 h of the beginning of simulation.

Table 1 shows the results of both the discrete and categorical statistical analysis detailed for each day of the episode of photochemical pollution. The model results achieve the USEPA (1991, 2005) goals for a discrete evaluation on all episode days. The O_3 MNBE is negative on each day, ranging from -2.1% on the first day of simulation to -14.3% on August 15. That suggests a slight tendency towards underprediction; however, USEPA goals of $\pm 15\%$ are achieved. This negative bias may suggest that the O_3 -production chemistry may not be sufficiently reactive. The UPA is overestimated on the first and last days of the simulations (14.4% and 5.2%, respectively) and underestimated on the central days of the episode (-3.8% and -11.7%). The MNGE increases from August 13 until August 16 (16.8–26.7%), mainly due to deviations in meteorological predictions that enlarge with the time of simulation (Jiménez et al., 2006). The objective set in the Directive 2002/3/EC (deviation of 50% for the 1-h averages) is also achieved for the whole period of study. With respect to categorical forecasting, statistical parameters indicate that the A (percent of forecasts that correctly predict an exceedance or non-exceedance) is around 90% for every day of simulation, decreasing the performance by the end of

the episode. The CSI and the POD yield more accurate values when O_3 peaks are higher. The value of B ($B < 1$ for all simulations) indicates that exceedances are generally underpredicted, which corresponds with the value of MNBE obtained for discrete evaluations. Last, the FAR is high for the first and last day of the simulations (around 68%), because of the possible initialization influence during the first moments of simulation that can be high for the sum of reservoir species for O_3 (Berge et al., 2001); and the errors attributable to the meteorology that accumulate over the period and perturb through the forecasts.

4. Conclusions

Although IC–BC specifications are recognized as an important issue in air quality modeling, systematic studies of their impacts are scarce. In this work, a description of the process of initialization and generation of BC for MM5–EMICAT2000–CMAQ through performing simulations in the entire Iberian Peninsula, and using a multiscale approach in order to provide the necessary boundaries for a domain in the NEIP. Furthermore, an analysis of the influences of IC–BC

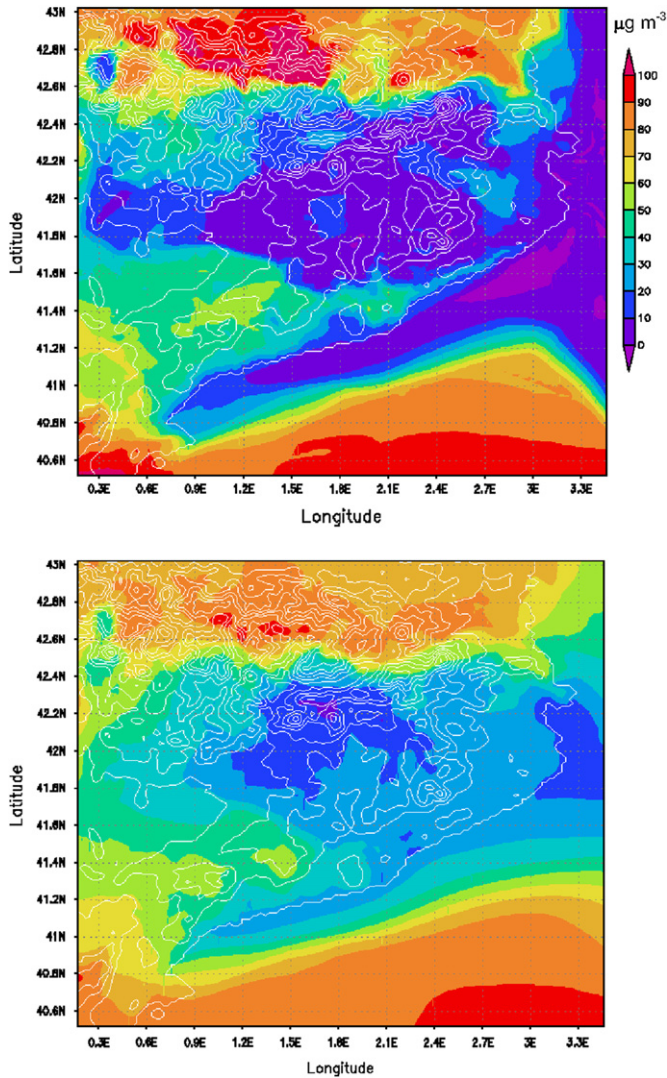


Fig. 11. Difference in the ground-level ozone ($\mu\text{g m}^{-3}$) results of the base simulation minus simulation with clean boundaries (Scenario 5) of D2 for the 72 h of the simulation: (top) difference in maximum 1 h concentrations and (bottom) difference in daily average concentrations (both in $\mu\text{g m}^{-3}$).

and their sensitivity on O_3 results is presented, indicating the necessity of a correct initialization of the model by means of spin-up procedures; and also the availability of good-quality boundary information when performing simulations in very complex terrains.

Results suggest that the impacts of IC on a given site decrease with simulation time and significantly affect the species concentrations before the arrival of BC, and are negligible after their arrival. Therefore, the influence of IC could be minimized through spin-up or start-up prior to formal simulations. Focusing on the conditions within the PBL, a 48-h spin-up time is sufficient to reduce the impact factor of IC to 10% or less for O_3 . Because of the model is initialized at 00.00 UTC, influence of the modification of O_3 precursors in the IC is very low during the night-time hours, increases until 30 h after the begin of the simulations and then decreases dramatically since the influence of pervasive local emissions that are much higher than the remaining contribution of initial precursors.

Table 1

Statistical measures of model performance for 1-h O_3 during the episode of August 13–16, 2000

	EPA goal	August 13, 2000	August 14, 2000	August 15, 2000	August 16, 2000
Discrete evaluation					
Observed peak ($\mu\text{g m}^{-3}$)		157	177	189	171
Modeled peak ($\mu\text{g m}^{-3}$)		189	170	167	180
UPA (%)	$<\pm 20\%$	14.4	-3.8	-11.7	5.2
MNBE (%)	$<\pm 15\%$	-2.1	-11.0	-14.3	-5.6
MNGE (%)	$<35\%$	16.8	19.8	21.7	26.7
Categorical evaluation					
A (%)		91.1	92.2	90.0	89.7
B (%)		0.7	0.1	0.1	0.4
POD (%)		22.1	6.9	9.6	11.5
CSI (%)		15.0	6.7	9.2	9.1
FAR (%)		67.9	33.3	31.3	69.6

The influence of BC is significant to a selected site when the arrival time of boundaries is short and the species lifetime is longer, as the case of O_3 . The impact of modifying boundary precursors in ground-level O_3 keeps under 20% during the whole period of simulations for most sites in the NEIP, since boundaries of the domain selected are far enough from relevant sites not to have a significant influence. The effect of modifying O_3 boundaries becomes evident after 30 h, when the impact factor of BC overcomes the value of 10% for ground-level O_3 , and dominates over the effect of IC after 35 h of the beginning of the simulation. Results indicate that influences of BC are more important for areas near domain boundaries, especially in background areas where contribution of O_3 precursors is due to a short-medium range transport.

In order to account for the advective transport through the boundary conditions to O_3 levels, simulations were conducted with clean BC respect to the base case simulations. The modeled O_3 indicates that the most important influence of advective transport is produced over the Mediterranean Sea. However, the particular conditions of the episode simulated (low pressure gradient meteorological conditions, with limitations in the advective transport and a strong dominance of the local emissions-photochemistry cycle) makes that the contribution of advective transport to maximum O_3 levels is just $4.7 \mu\text{g m}^{-3}$, which signifies just a 2.5% of the final maximum concentrations.

Finally, it should be highlighted that, despite the influence of IC may be minimized through a proper spin-up time of 48 h, the importance of BC becomes essential and their contribution in O_3 concentrations over the domain increase with the time of simulation. Therefore, it is necessary to carefully consider this issue when applying air quality models. In this work, this problem is resolved by including all the sources that have potential effects on the given region in the domain of the NEIP; and by applying the nested simulation results of a larger model domain covering the entire Iberian Peninsula to the BC of smaller nested simulation domain.

Acknowledgements

This work was developed under the research contract REN2003-09753-C02 of the Spanish Ministry of Science and Technology. The Spanish Ministry of Education and Science is also thanked for the FPU doctoral fellowship hold by P. Jiménez. The authors gratefully acknowledge O. Jorba for providing meteorological inputs and E. López for the implementation of EMICAT2000 into a GIS system. Air quality stations data and information for implementing industrial emissions were provided by the Environmental Department of the Catalonia Government (Spain).

References

- Byun, D.W., Ching, J.K.S. (Eds.), 1999. Science Algorithms of the EPA Models-3 Community Multiscale Air Quality (CMAQ) Modeling System. EPA Report N. EPA-600/R-99/030, Office of Research and Development. U.S. Environmental Protection Agency, Washington, DC.
- Berge, E., Huang, H.-C., Chang, J., Liu, T.-H., 2001. A study of the importance of initial conditions for photochemical oxidant modeling. *Journal of Geophysical Research* 106 (D1), 1346–1363.
- Dudhia, J., 1993. A nonhydrostatic version of the Penn State/NCAR mesoscale model: validation tests and simulation of an Atlantic cyclone and cold front. *Monthly Weather Review* 121, 1493–1513.
- Gangoiti, G., Millán, M.M., Salvador, R., Mantilla, E., 2001. Long-range transport and re-circulation of pollutants in the western Mediterranean during the project regional cycles of air pollution in the west-central Mediterranean area. *Atmospheric Environment* 35, 6267–6276.
- Gery, M.W., Whitten, G.Z., Killus, J.P., Dodge, M.C., 1989. A photochemical kinetics mechanism for urban and regional scale computer modeling. *Journal of Geophysical Research* 94 (D10), 12925–12956.
- Hogrefe, C., Rao, S.T., Kasibhatla, P., Hao, W., Sista, G., Mathur, R., McHenry, J., 2001. Evaluating the performance of regional-scale photochemical modeling systems: part II – ozone predictions. *Atmospheric Environment* 35, 4175–4188.
- Huang, H.-C., Chang, J.S., 2001. On the performance of numerical solvers for a chemistry submodel in three-dimensional air quality models. *Journal of Geophysical Research* 106, 20175–20188.
- Jiménez, P., Baldasano, J.M., 2004. Ozone response to precursor controls in very complex terrains: use of photochemical indicators to assess O_3 – NO_x –VOC sensitivity in the northeastern Iberian Peninsula. *Journal of Geophysical Research* 109, D20309, doi:10.1029/2004JD004985.
- Jiménez, P., Parra, R., Gassó, S., Baldasano, J.M., 2005. Modeling the ozone weekend effect in very complex terrains: a case study in the northeastern Iberian Peninsula. *Atmospheric Environment* 39, 429–444.
- Jiménez, P., Jorba, O., Parra, R., Baldasano, J.M., 2006. Evaluation of MM5–EMICAT2000–CMAQ performance and sensitivity in complex terrain: high-resolution application to the northeastern Iberian Peninsula. *Atmospheric Environment* 40 (26), 5056–5072, doi:10.1016/j.atmosenv.2005.12.060.
- Jorba, O., Pérez, C., Rocadenbosch, F., Baldasano, J.M., 2004. Cluster analysis of 4-day back trajectories arriving in the Barcelona area (Spain) from 1997 to 2002. *Journal of Applied Meteorology* 43, 887–901.
- Kang, D., Eder, B.K., Schere, K.L., 2003. The evaluation of regional-scale air quality models as part of NOAA's air quality forecasting pilot program. In: 26th NATO International Technical Meeting on Air Pollution Modeling and its Application, Istanbul, Turkey, 404–411.
- Kang, D., Eder, B.K., Mathur, R., Yu, S., Schere, K.L., 2004. An operational evaluation of the ETA-CMAQ air quality forecast model. In: 27th NATO International Technical Meeting on Air Pollution Modeling and its Application, Banff, Canada, 233–240.
- Liu, T.-H., Jeng, F.-T., Huang, H.-C., Berge, E., Chang, J.S., 2001. Influences of initial and boundary conditions on regional and urban scale Eulerian air quality transport model simulations. *Chemosphere – Global Change Science* 3, 175–183.
- Millán, M.M., Artiñano, B., Alonso, L., Castro, M., Fernandez-Patier, R., Goberna, J., 1992. Mesometeorological Cycles of Air Pollution in the Iberian Peninsula. In: Air Pollution Research Report 44. Commission of the European Communities, Brussels, Belgium, 219 pp.
- Millán, M.M., Salvador, R., Mantilla, E., Artiñano, B., 1996. Meteorology and photochemical air pollution in southern Europe: experimental results from EC research projects. *Atmospheric Environment* 30, 1909–1924.
- Millán, M., Salvador, R., Mantilla, E., Kallos, G., 1997. Photooxidant dynamics in the Mediterranean basin in summer: results from European research projects. *Journal of Geophysical Research* 102, 8811–8823.
- National Research Council, 1991. Rethinking the Ozone Problem in Urban and Regional Air Pollution. National Academy Press, Washington, DC.
- Ntziachristos, L., Samaras, Z., 2000. COPERTIII, Computer Programme to Calculate Emissions from Road Transport. Methodology and Emission Factors (Version 2.1). Technical report No 49. European Environment Agency.
- Parra, R., Jiménez, P., Baldasano, J.M., 2006. Development of the high spatial resolution EMICAT2000 emission model for air pollutants from the north-eastern Iberian Peninsula (Catalonia, Spain). *Environmental Pollution* 140, 200–219.
- Parra, R., Gassó, S., Baldasano, J.M., 2004. Estimating the biogenic emissions of non-methane volatile organic compounds from the North western Mediterranean vegetation of Catalonia, Spain. *Science of the Total Environment* 329, 241–259.
- Pérez, C., Sicard, M., Jorba, O., Comerón, A., Baldasano, J.M., 2004. Summertime re-circulations of air pollutants over the north-eastern Iberian coast observed from systematic EARLINET lidar measurements in Barcelona. *Atmospheric Environment* 38, 3983–4000.
- Pérez, C., Jiménez, P., Jorba, O., Sicard, M., Baldasano, J.M., 2006. Influence of the PBL scheme on high resolution photochemical simulations in an urban coastal area over the Western Mediterranean. *Atmospheric Environment* 40 (27), 5274–5297, doi:10.1016/j.atmosenv.2006.04.039.
- Pineda, N., Jorba, O., Jorge, J., Baldasano, J.M., 2004. Using NDVI SPOT-VGT data to update land-use map: application to a mesoscale meteorological model. *International Journal of Remote Sensing* 25 (1), 129–143.
- Russell, A., Dennis, R., 2000. NARSTO critical review of photochemical models and modeling. *Atmospheric Environment* 34, 2283–2324.
- Sokhi, R.S., San José, R., Kitwiroon, N., Fragkou, E., Pérez, J.L., Middleton, D.R., 2006. Prediction of ozone levels in London using the MM5CMAQ modelling system. *Environmental Modelling & Software* 21 (4), 566–576.
- Seinfeld, J.H., Pandis, S.N. (Eds.), 1998. *Atmospheric Chemistry and Physics: From Air Pollution to Climate Change*. Wiley-Interscience, New York, 1326 pp.
- San José, R., Pérez, J.L., González, R.M., 2007. An operational real-time air quality modelling system for industrial plants. *Environmental Modelling & Software* 22 (3), 297–307.
- Soriano, C., Jorba, O., Baldasano, J.M., 2002. One-way nesting versus two-way nesting: does it really make a difference? In: Borrego, C., Suyches, G. (Eds.), *Air Pollution Modeling and its Applications XV*. Kluwer Academic/Plenum Publishers, pp. 177–185.
- USEPA, 1991. Guideline for Regulatory Application of the Urban Airshed Model. US EPA Report No. EPA-450/4-91-013. Office of Air and Radiation, Office of Air Quality Planning and Standards, Technical Support Division, Research Triangle Park, North Carolina, US.
- USEPA, October 2005. Guidance on the Use of Models and Other Analyses in Attainment Demonstrations for the 8-hour Ozone NAAQS. US EPA Report No. EPA-454/R-05-002. Office of Air Quality Planning and Standards, Research Triangle Park, North Carolina, US, 128 pp.
- Zhang, M., Pu, Y., Zhang, R., Han, Z., 2006. Simulation of sulfur transport and transformation in East Asia with a comprehensive chemical transport model. *Environmental Modelling & Software* 21 (6), 812–820.
- Zunckel, M., Koosailee, A., Yarwood, G., Maure, G., Venjonoka, J., van Tienhoven, A.M., Otter, L., 2006. Modelled surface ozone over southern Africa during the Cross Border Air Pollution Impact Assessment Project. *Environmental Modelling & Software* 21 (7), 911–924.